Toward mechanical recyclability of high barrier food packaging films through filler incorporation on the EVOH layer

Carolina Barros [1,2] © | Ana G. Azevedo [3] ® | Miguel A. Cerqueira [3] © | O. S. Carneiro [1] (○) | A. V. Machado [1] (○)

[1] Institute for Polymers and Composites (IPC), University of Minho, Guimarães, Portugal
[2] Research Centre, Centre for Innovation in Polymer Engineering (PIEP), Guimarães, Portugal
[3] Research Centre, International Iberian Nanotechnology Laboratory (INL), Braga, Portugal

Funding information

European Regional Development Fund, Grant/Award Number: POCI-01-0247-FEDER-046091

Abstract

To preserve food from moisture and oxygen, polymers, such as ethylene vinyl alcohol (EVOH) are used in multilayer structures to provide oxygen barrier, while low-density polyethylene (LDPE) is used for a water vapor barrier. While this material combination is functionally ideal, it may not comply with the new packaging recycling guidelines. Some European markets have implemented rules that limit the weight percentage of EVOH in LDPE films. One way to increase recyclability is by reducing the amount of EVOH in the film structure while maintaining the packaging's oxygen barrier properties. To achieve this, it is necessary to improve the barrier properties of EVOH. With this objective in mind, this study evaluated the incorporation of nanoclays (NC), cellulose microcrystals (MCC), silicon dioxide nanoparticles (SiO_2), and cellulose nanocrystals (CNC) into an EVOH matrix. The results indicate that NC and MCC facilitate a stable blown film extrusion process and have a better dispersion in the EVOH matrix. Based on this finding, three-layer films (with an ABA configuration) consisting of LDPE (A) and EVOH ($7\ \mu\ m$ layer) with 0.5 or 1 $wt.\%$ MCC or NC (B) were produced to protect the

EVOH from moisture and enable blown film processing. The oxygen transmission rate (OTR) values were lowest for $0.5\,wt.\%NC$ and $1\,wt.\%$ MCC incorporation. Although the films with micro and nanoparticles had increased haze, this did not affect the visibility of the packaged food.

KEYWORDS

barrier properties, blown film, microcrystalline cellulose, montmorillonite, nanomaterial

1 | INTRODUCTION

One of the most important properties of food packaging films is their ability to prevent permeability to oxygen and water vapor, which slows lipid oxidation and the growth of mold and fungi in the food. This double barrier in flexible plastic packaging is achieved by combining
different polymers in a multilayer structure, where polymers, such as polyethylene (PE) or polypropylene (PP) constitute the water vapor barrier, and ethylene vinyl alcohol (EVOH) or polyamide (PA) serve as oxygen barrier. [1] Unfortunately, this combination of polymers does not allow to recycle the films at the end of its life time. [2]

The incompatibility between the PE , or PP , and EVOH, or PA, layers makes it mandatory to use a compatibilizer between these layers. [3] Given the current packaging sorting and recycling methods, it is nearly impossible to separate these materials at the packaging end-of-life. Many recyclers consider plastic packaging recyclable if $95\,wt.\%$ of its composition is made of the same material, or if the density of a flexible polyolefin film is not higher than $0.97\ \ g/cm^3$. [4–6] Therefore, if monomaterial packaging is not an option, it is necessary to keep the inclusion of different materials to a maximum of $5\,wt.\%$.

One of the strategies for reducing the amount of other polymers used in a package involves replacing some layers with composite or nanocomposite materials. For example, in a film mainly composed of LDPE, incorporating micro- and nanoparticles into the EVOH inner layer can enhance its properties, allowing for a decrease in layer thickness and, consequently, reducing the proportion of EVOH in the film. Several studies demonstrate that composites, especially nanocomposites, improve the mechanical and barrier properties of flexible plastic films, while also showing good stability at different temperatures. [7,8]

Polymer nanocomposites with good dispersion and distribution of nanoparticles exhibit better thermal, mechanical, and optical properties when compared to virgin polymer and microcomposites. [9–11]

There are several studies on the incorporation of nanoparticles in EVOH matrices, with the aim of improving the properties of this polymer for use in food packaging. The chemical structure of EVOH, consisting of polar segments, vinyl alcohol, and nonpolar segments of ethylene, improves the EVOH/particle bond through hydrogen bonding interactions. [12,13] For this reason, in several studies related to the production of EVOH matrix nanocomposites, the use of a compatibilizer is not detected. [14–17]

Nanoclays (NC) are currently one of the most widely used materials for the production and development of nanocomposites in the field of food packaging. There are several types of mineral clays namely chlorite, montmorillonite (MMT), illite, and kaolinite, which differ in chemical structure, composition, and source. Of all types of nanoclays, MMT are the best known and most used in the packaging area, mainly to improve oxygen barrier and mechanical properties. [18,19] Studies carried out on the effect of NC on the properties of EVOH nanocomposites show that the NC incorporation helps in reducing the permeability to oxygen and water vapor, and increases the glass transition temperature (T_g), melting temperature (T_m), and percentage of crystallinity (X_m) . [15,20−22] Increasing the incorporation rate of NC in the EVOH matrix has advantages for the permeability and thermal
stability of the nanocomposite, but above $5\,wt.\,\%$ leads to a decrease in film transparency, which is an important requirement for food packaging films. [22]

Regarding CNC, the incorporation of only $1\,wt.\,\%$ of these nanoparticles in an EVOH matrix allows to obtain a 71% decrease in the water vapor transmission rate and an increase in T_g, T_m, X_m, and mechanical properties when compared to a 100 % EVOH film. [23,24]

Recent studies compare EVOH composites produced with MCC and CNC and evaluate the effect of shear forces on the dispersion of micro and nanoparticles during the production of the composites by extrusion. Ethylene vinyl alcohol microcomposites with 5 and $15\,wt.\,\%$ MCC prepared with a high shear screw configuration exhibit better mechanical and thermal properties than microcomposites produced with a low shear screw configuration. [17] The properties improvement of the microcomposite with $5\,wt.\,\%MCC$ is not significantly different from that corresponding to the nanocomposite with the same percentage of CNC incorporation. [17] Therefore, the incorporation of MCC into a polymeric matrix can be a low-cost alternative to replace the use of CNC when using melt compounding as a dispersive method of particles in a polymeric matrix.

Also nano- SiO_2, widely used as an antiblocking additive, can be used in flexible food packaging to improve barrier, antimicrobial and mechanical properties. [25,26] Liu et al. (2010) demonstrate that the incorporation of nanoSiO_2 into an EVOH matrix decreases the moisture permeability and increases the film tensile strength. Above $2\,wt.\,\%$ of incorporation of nano- SiO_2, the increase in tensile strength is not noticeable, but the decrease in the moisture permeability coefficient increases considerably with the incorporation of $5\,wt.\,\%$. The same authors conclude that to reduce the turbidity associated with the increase in wt. % of nano- SiO_2, the take-up ratio (TUR) used in the film extrusion line should be increased. [16]

In spite of the studies published in the literature, none have used samples manufactured through coextrusion, the industry's most prevalent processing technique. Furthermore, there is a lack of comprehensive studies on the incorporation of several types of microand nanoparticles in the EVOH layer of multilayer films.

The micro- and nanoparticles used in the current research have been approved for food contact by commission Reg. (EU) No. 10/2011 dated January 14, 2011, with the exception of CNC. Cellulose nanocrystals have a smaller particle size than microparticles, which

can result in different toxicological properties. However, further studies are needed to assess their behavior as food contact material. [27,28]

Considering these findings, the focus of the current research is the incorporation of four types of micro- and
nanoparticles in the EVOH layer with a view to produce multilayer food packaging films with improved properties, namely oxygen barrier. These particles are: CNC, MCC, NC, and SiO_2. The micro and nanocomposites were prepared by extrusion compounding and the respective films were produced through blown film coextrusion.

The work is divided into two parts. Initially, the dispersion of micro- and nanoparticles and the properties of the EVOH film and its nanocomposites were investigated. After this analysis, films with three layers (LDPE|EVOH|LDPE) were produced. The outer layers were made of LDPE, a hydrophobic non-polar polymer, while the inner layer was made of EVOH or its micro and nanocomposites. The support provided by the two LDPE layers during blown film extrusion allowed for a reduction in the thickness of the EVOH layer to 7 $\mu\ m$, a value similar to that used in commercial films. The LDPE layers also played a crucial role in limiting the diffusion of water vapor into the EVOH layer, thereby maintaining its oxygen barrier characteristics.

2 | EXPERIMENTAL

1 | Materials

Ethylene vinyl alcohol Soarnol DC3203RB, from NIPPON GOHSEI (Osaka, Japan), containing 32 $mol\%$ of ethylene (density ¿ 1.19 g/cm^3, melt temperature ¿ 83 $^\circ C$, and MFI $(210^\circ C, 2.16\ kg) = 3.8\ g/10\ min)$ was used as matrix. Dow (Michigan, EUA) LDPE 352 E, a low-density
polyethylene blown film extrusion grade (densi$ty = 925\ kg/m^3$, MFI $(190^\circ C/2.16\ kg) = 2.0\ g/10\ min$ and Vicat softening temperature ¿ 96.0 $^\circ C$) was used for coextrusion purposes. The NC used was Cloisite 20A, from BYK (Wesel, Germany), which is a MMT with organic modifier dimethyl, dihydrogenated tallow, quaternary ammonium, and a particle size of 2 to 13 $\mu\ m$. The CNC (reference NCV100) was supplied by CelluForce (Montreal, Canada). This is a cellulose hydrogen sulphate sodium salt with a particle size of 1 to 50 $\mu\ m$. The MCC Vivapur 105, was supplied by J. Rettenmaier & Sohne (Rosenberg, Germany) and has a medium size particle of 15 $\mu\ m$. The SiO_2 avanSi-40 was supplied by Avanzare (La Rioja, Spain) and has a medium size particle of 3.5 $\mu\ m$. Additional relevant information obtained from the technical data sheets of the micro- and nanoparticles can also be found in Table 1.

2 | Masterbatch preparation

Ethylene vinyl alcohol masterbatches with NC, SiO_2, MCC, and CNC were produced for posterior dilution in EVOH and film production. These materials were processed in a model ZSK 26 Coperion co-rotating twinscrew extruder ($L/D = 40, D = 25\ mm$), with 10 independent heating zones, and a screw configuration including five distinct mixing

zones, composed by kneading blocks staggered at $30^{\circ}, 45^{\circ}$, and 90°, separated by conveying zones. Initially, the masterbatches were produced with $20\,wt\,\%$ particle incorporation, using a temperature of

TABLE 1 Technical properties of CNC, MCC, NC, and SiO_2.

CNC				
Particle size (μm)	Zeta potential (mV)	Specific surface area (m^2/g)	Sulfur content (%)	Sulfate content (mmol/kg)
1-50	-37	400	0.86-0.89	246-261
MCC				
Particle size (μm)	pH		Conductivity ($\mu S/cm$)	
15	5.0-7.0		75	
NC				
Particle size (μm)	Loss On Ignition (%)		X-Ray Diffraction d-Spacing (001) (Å)	
$10\% \leq 2.0\mu\ m, 50\% \leq$, $90\% \leq 13\mu\ m$	38		31.5	
SiO_2				
Particle size (μm)	pH		Loss On Ignition (%)	
3.5	11-12		21	

$210^{\circ}C$ (in zones 1, 2, 3, 4, 9, and 10) and $200^{\circ}C$ (in zones 5, 6, 7, and 8), with screws rotation speed of 180 rpm . Before compounding, all micro- and nanoparticles and EVOH were dried for 24 h at $55^{\circ}C$ in a forced convection oven.

The EVOH was fed to the extruder hopper using a single-screw gravimetric feeder K-Tron K-CL-24-KQX4, and the micro- and nanoparticles were fed by a doublescrew volumetric K-Tron K- CL-24-KT20 side feeder, located in zone 5. This downstream location was intended to reduce the particles residence time in the extruder, preventing their thermal degradation. With this percentage of incorporation ($20\,wt\,.\,\%$), all particles except NC presented problems during extrusion, namely: nonuniform extruded filament diameter in SiO_2 nanocomposites, and visible thermal degradation (darkening of the composites) of micro and MCC and CNC nanocomposites. To overcome this issue, $EVOH/SiO_2$, $EVOH/MCC$, and EVOH/CNC masterbatches were produced only with

the incorporation of 10 $wt.\%$, with a temperature profile of $190^{\circ}C$ (zones 1-4) and $180^{\circ}C$ (zones 5-10).

3 | EVOH film production

In order to produce single layer EVOH micro and nanocomposite films, co-extruded LDPE|EVOH blown film samples were produced using two Periplast single screw extruders, $L/D=25$ and $D=25$, coupled to a two-layer co-extrusion head. The Extruder 1 processed the EVOH or the EVOH micro and nanocomposites, diluting the masterbatch, and Extruder 2 processed LDPE. The use of the LDPE layer was required to enable the production of an EVOH film, since this polymer does not have sufficient melt strength (extensional viscosity) to form a stable bubble during the blown film process. Although EVOH is incompatible with LDPE, no compatibilizer was used, because the aim is to analyze the behavior of the EVOH layer and not that of the two layers film. The monolayer EVOH and EVOH composite films were obtained by separating the EVOH layer from the incompatible LDPE layer, by simply pulling it off.

The Extruder 1 temperature profile was set at $200-¿\,210-210^{\circ}C$ (except for nanocomposites with NC, where the profile was $210-230-220^{\circ}C$). The Extruder 2 temperature profile was set at $170-180-195-200^{\circ}C$, and the extrusion head were set at $210^{\circ}C$. A blow-up ratio (BUR) of 2.0 and a 10.6 take-up ratio (TUR) were used in the films production. The films thickness was measured with a micrometer (Digimatic thickness gage 547-301, Mitutoyo, Japan) with a measuring accuracy of 0.01 mm . The final film thickness ranged from 22 to 40 μm. In total, 17 films were produced, including one with neat EVOH, using four different incorporation rates of each type of micro- and nanoparticles (0.5, 1.0, 2.5, and 5.0 $wt.\%$) in the EVOH layer.

Due to the high thickness of the EVOH film obtained through the process described (around 30 μm), and despite the presence of the LDPE layer, it was not possible to keep the extruded bubble stability. As a consequence, the films obtained had many creases and a pronounced thickness distribution, in both machine direction (MD) and transverse direction (TD).

4 | Three-layer LDPE|EVOH|LDPE film production

The previous stage of this research enabled the selection of the best nanocomposites for incorporation in threelayer films. These films were produced with an ABA configuration (LDPE|EVOH|LDPE), with NC and MCC incorporated in the inner EVOH (B) layer at 0.5 and 1.0 $wt.\%$, obtained by diluting the masterbatches produced. The five films were named as follows:

1. LDPE | EVOH | LDPE
2. LDPE|EVOH +0.5 $\%NC$ | LDPE
3. LDPE |EVOH +1.0 $\%NC$ | LDPE
4. LDPE|EVOH +0.5 % MCC|LDPE

5. LDPE | EVOH +1.0% MCC|LDPE.

The production of these films was carried out with a temperature profile of 180 to $190^{\circ}C$, in the LDPE extruder, $200^{\circ}C$ in the EVOH extruder and $200^{\circ}C$ in the co-extrusion head. A BUR of 1.7 and TUR of 13.8 were used. The total thickness of these films varied from 60 to $70\,\mu m$. Having in mind that the melt mass flow rate at the die exit and the mass flow rate of the final solid film are the same (due to mass conservation), the total stretch ratio (BUR multiplied by TUR) required to achieve the typical thickness of the EVOH layer in industrial films (around $7\,\mu m$) was computed.

5 | Characterization techniques

1 | Scanning electron microscopy

Scanning electron microscopy (SEM) analysis allowed to observe the morphology of the samples using a scanning electron microscope (Quanta 650 FEG, FEI, USA) with an operating voltage of 5 kV .

2 | Optical properties

The films haze was determined in a XL-211 Hazegard System transmittance meter, according to ASTM D1003-00. For each sample, five measurements were performed.

Films gloss measurements were performed according to ISO 2813 standard using a BYK Micro-TRI-gloss S gloss meter, with 20° and 60° measurement geometries. The analysis of particle distribution in EVOH monolayer films was done using a digital microscope with a low to medium magnification range, Leica DMS1000, with image collection through LAS EZ software in three different zones of the film.

3 | Barrier properties

The oxygen transmission rate (OTR) tests were carried out on a OTR analyzer OX-TRAN model 2/21 from MOCON, using a coulometric sensor. The multilayer films were tested at two values of relative humidity (RH: 0% and $RH: 60\%$), at a temperature of $23^{\circ}C$. This test was carried out in accordance with the ASTM D 3985 standard.

The water vapor transmission rate (WVTR) tests were performed according to the desiccant method from ASTM E96/E96M-10. The samples with 8 cm diameter were sealed to the open mouth of a test cup, containing calcium chloride pre-dried at $200^{\circ}C$. The samples were placed inside a desiccator at $23 \pm 2^{\circ}C$ and weighed every 24 h for a period of 25 days for monolayer films, and 50 days for multilayer films. The samples were weighted on an analytical balance, with a 1 mg sensitivity. The WVTR is the slope obtained by fitting the weight change over time via a linear regression.

4 | X-ray diffraction

X-ray diffraction (XRD) system (Malvern Panalytical Ltd., Malvern, UK) was used to evaluate the crystallographic structure of MCC. PANanalytical X'Pert HighScore Plus was the software used to gather data and to analyze peak diffractions. The film samples were

fixed by a tape in the sample holder. The XRD diffractograms were acquired at $23 \pm 2^{\circ} C$. Angular scans from 5° to 50° (2θ) were performed with a Cu source, X-ray tube ($\lambda = 1.54056$ Å) at 45 kV and 40 mA. The fine calibration offset for 2θ was -0.0372°. One measurement was performed in each sample.

Small angle X-ray scattering (SAXS) measurements were carried out to characterize the structural and
crystallinity changes over time of nanoclays (NC) films. The samples were measured with a SAXSess mc^2 Kratky camera (Anton Paar GmbH, Austria) using CuKaradiation ($\lambda = 1.54056$ Å) and operating at 40 kV and 50 mA. An image plate system covering the q-range from 0.23 to 26 nm^{-1} was used. The exposure time for all samples was 60 min being the temperature $25^{\circ} C$. The measurements were performed in line collimation mode to maximize scattering intensity. The 2D scattering images were converted to 1D radial intensity profiles using the SAXS-quant software (Anton Paar GmbH, Austria).

5 | Thermogravimetric analysis

Thermogravimetric analysis (TGA) of the micro- and nanoparticles was performed on a TGA Q500 (TA Instruments, New Castle, EUA) at $10^{\circ} C/min$ in a temperature range of $40 - 700^{\circ} C$, under a nitrogen atmosphere. The extrapolated onset temperature (where the weight loss begins), the maximum weight loss temperature, and the total weight loss were calculated.

6 | Statistical analyses

The results of OTR, WVTR and haze measurements are provided in the mean ± standard deviation format. The statistical analysis was carried out using the software IBM SPSS Statistics, using a one-way analysis of variance (ANOVA), with comparison procedures assuming equal variances with Tukey method for differences of means, with a confidence level of 95%.

3 | RESULTS AND DISCUSSION

1 | Dispersion and barrier properties of micro and nanoparticles in EVOH films

Micro and nanoparticles were subjected to TGA to investigate their stability when subjected to the EVOH processing temperatures $(190 - 200^{\circ} C)$. The results in Table 2 indicate that, with the exception of SiO_2, the initial weight loss occurs at temperatures above $200^{\circ} C$. SiO_2 start to loss weight and the degradation temperature occurs between 100 and $200^{\circ} C$, which can be attributed to the physisorbed water in SiO_2 particles. [29,30] However, SiO_2 particles have the lowest total weight loss and are the only ones that maintain their original color (white) even when exposed to high temperatures (up to

700˚C). NC exhibited a weight loss of 31.49 %, which is associated to the presence of organic groups used to modify the

TABLE2 TGA results of CNC, MCC, NC, and SiO_2.

Materials	Initial decomposing temperature (˚C)	1st derivate peak temperature (˚C)	Residue (%)
CNC	299	308	4
MCC	319	343	3
NC	263	314	69
SiO_2	83	127	82

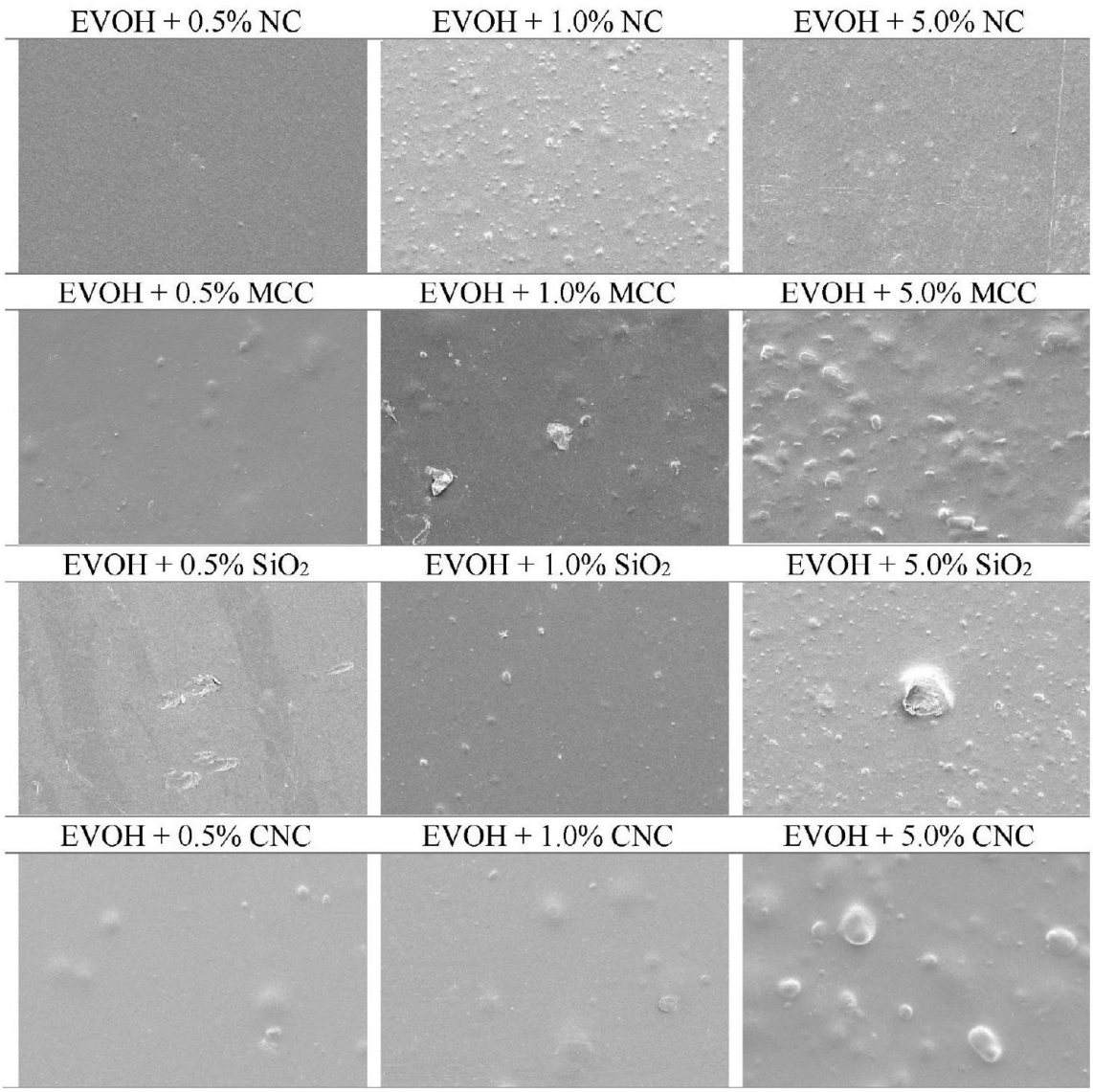

FIGURE 1 SEM micrographs, with a 750 × magnification, of the surface of EVOH films incorporating NC, MCC, SiO_2, and CNC.
natural clays and increase the interlamellar distance, and was also observed by Voorn et al. (2006). [31]

The SEM images of the samples surface (Figure 1) exhibited a high number of agglomerates and deterioration of the film surface, in the MCC, SiO_2, and CNC composites, which is intensified when the incorporation rate increases. The MCC agglomerates are smaller in size, than the SiO_2 and CNC ones, and are better distributed.

Although the selected MCC has low conductivity and a neutral pH , indicating that electrostatic forces are not significant for its dispersion, it also has a lower surface area to volume ratio than nanoparticles, and therefore, it has a lower tendency for agglomeration. [32]

The NC composite films show better dispersion and distribution of these particles when compared to the remaining films. Their interlayer modification with

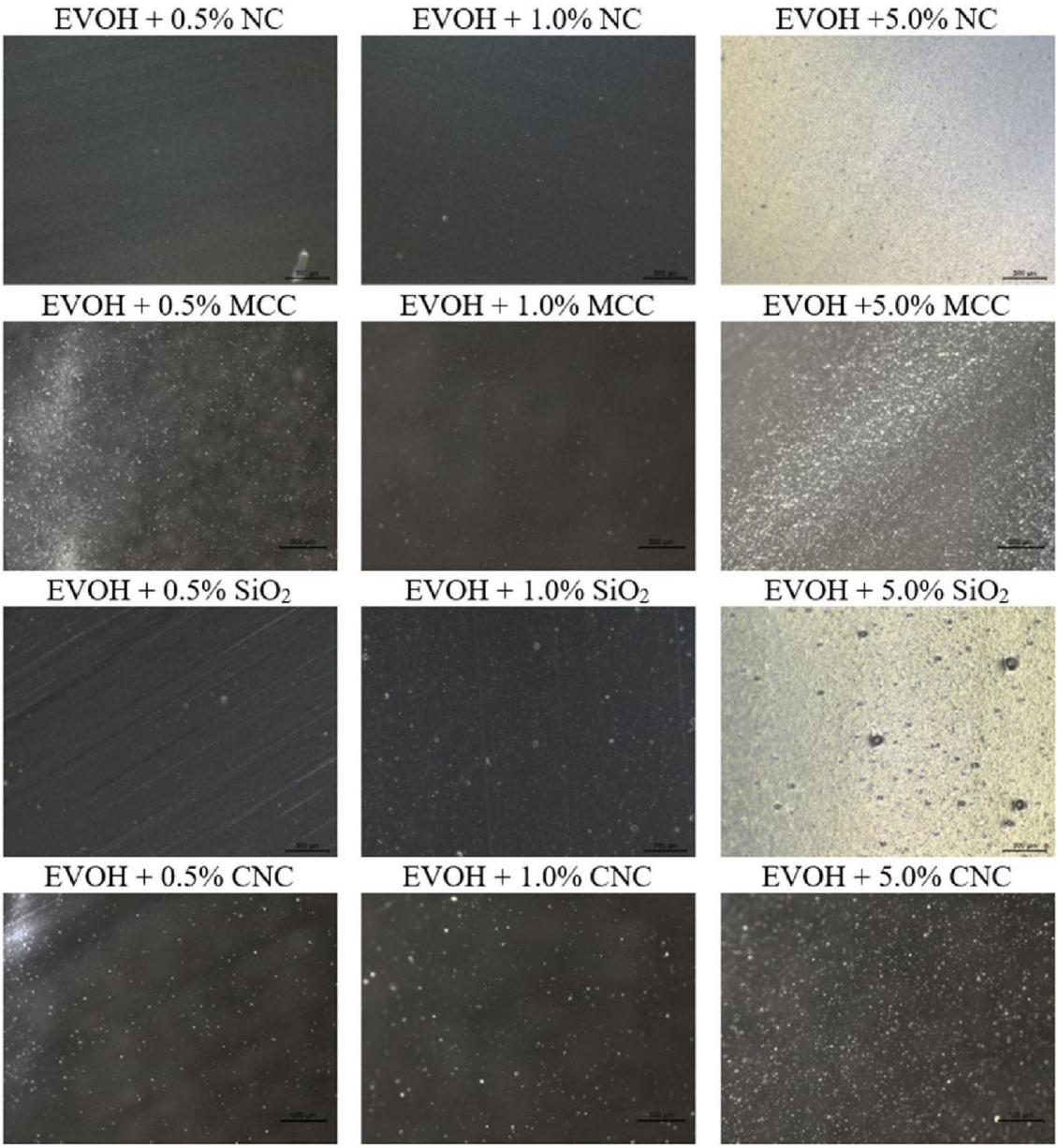

FIGURE 2 Surface images of EVOH films incorporating NC, MCC, SiO_2, and CNC through microscopy with a 3.22 × magnification. [Color figure can be viewed at wileyonlinelibrary.com]

quaternary ammonium introduces positive charges that can interact with polar or negatively charged groups in the EVOH matrix, facilitating dispersion through electrostatic attractions. Organic modification reduces the surface energy of nanoclays, lowering agglomeration and promoting uniform dispersion in the polymer matrix.

For the composite films containing 5.0 wt % of MCC, CNC , and SiO_2, the presence of large agglomerates is observed, which negatively impacts the surface roughness of the films. Additionally, it is important for the size of the agglomerates to not exceed the typical thickness range of the EVOH layer ($3-7\mu\ m$) in food packaging films. [33]

Regarding CNC dispersion, the sulfate groups on their surface introduce negative charges resulting in a negative zeta potential (-37 mV). These electrostatic forces between negatively charged CNC and the EVOH matrix can facilitate uniform dispersion if the matrix contains polar or charged functional groups. [34] However, agglomerates of these particles can be seen in all the films with CNC incorporation (Figures 1 and 2). These effects can be attributed to the strong attraction between CNCs, promoted by the hydroxyl groups (OH) on their surface, as well as their large surface area and high surface energy, which cause aggregation. [35]

For SiO_2, although alkaline pH may influence its interaction with the EVOH matrix, and a calcination loss of 21 % may indicate possible surface modification, this did not overcome its high surface energy, as evidenced by the presence of aggregates in the produced films.

Figure 2 shows the digital microscope images of the monolayer films surface showing the particle distribution. In most formulations, the incorporation of 5.0 wt . % of micro and nanoparticles into the EVOH matrix leads to a visible increase in particle agglomerates on the surface of the films, except for films with NC. The surface images of the NC formulations are similar, even for the higher concentrations. This effect may be related to the better dispersion of these particles, as observed in the SEM images (Figure 1). The films that showed more surface defects were clearly those containing MCC and CNC. The formation of bubbles was observed during the production of these films, which may be associated with the humidity existing in these particles, as observed by Graninger et al. (2020) and Santos et al. (2013), despite their prior drying before masterbatch and film production. [17,36] The poor dispersion of these particles can also induce bubble instability during extrusion, causing its rupture where agglomerates exist, as observed by Santos et al. [36] and also noticed during the extrusion of the 5.0 % MCC and 5.0 % CNC formulations. Since SiO_2 is widely used in films as an anti-blocking agent, especially in PP and PE matrices, a high surface roughness would be expected for these composite films; in fact, particles/ agglomerates of SiO_2 are easily observed in the EVOH +5.0 % SiO_2 film. [37]

As expected, all composite films exhibited higher turbidity than the EVOH film and an increase in haze as the incorporation rate of nano and microparticles increases, as can be seen in Table 3. This is in agreement with the observations made by microscopy. The EVOH +0.5 SiO_2, EVOH +1.0 % SiO_2, and EVOH +0.5 % CNC films have turbidity values closer to that of EVOH film. EVOH composite films with CNC exhibited the highest haze values, reaching up to 19.0 % when incorporating 5 wt % CNC. This aligns with the presence of large agglomerates, which effectively scatter light and increase haze. These results indicate that low incorporation rates of nanoparticles originate their better dispersion and distribution in the matrix, leading to fewer aggregates and better light transmission as it was also observed by Mountain & Keating (2021) and Yao et al. (2014). [38,39]

The WVTR results of EVOH monolayer films (which, as previously stated, have an average thickness of 30 μm), were inconclusive due to the wide variation of thickness obtained (of the order of 40 %). This can be associated to the instability occurred in the extrusion process, since the bubble presented a pronounced diameter variation and,

TABLE 3 Haze of pure EVOH and the EVOH micro and nanocomposites films.

Monolayer film samples	Haze (%)
EVOH	7.7 ± 0.2^{F}
EVOH +0.5% NC	12.8 ± 0.8^{D}
EVOH +1.0% NC	14.9 ± 1.6^{c}
EVOH +2.5% NC	16.4 ± 0.0^{B}
EVOH +5% NC	16.5 ± 0.0^{B}
EVOH +0,5% MCC	15.2 ± 0.7^{c}
EVOH +1% MCC	16.5 ± 0.0^{B}
EVOH +2.5% MCC	16.6 ± 0.0^{B}
EVOH +5% MCC	16.8 ± 0.0^{B}
EVOH $+0.5\% SiO_2$	9.2 ± 0.7^{E}
EVOH $+1\% SiO_2$	9.6 ± 0.5^{E}
$EVOH + 2.5\% SiO_2$	16.6 ± 0.0^{B}
EVOH $+5\% SiO_2$	16.6 ± 0.0^{B}
EVOH +0.5% CNC	9.8 ± 0.2^{E}
EVOH +1% CNC	12.7 ± 0.2^{D}
EVOH +2.5% CNC	18.7 ± 0.0^{A}
EVOH +5% CNC	19.0 ± 0.1^{A}

Note: Means that do not share a letter are significantly different.
consequently, a wide thickness distribution in both MD and TD. During the delamination of the EVOH and LDPE layers, the EVOH frequently tore and broke. This is not surprising since this material is used as an oxygen barrier, being inadequate for incorporation in structural layers.

The OTR values exceeded the maximum limit of the equipment ($200\ \ cm^3/m^2$ day, unmasked) for most composite films and the few results achieved were not consistent. This may also be due to the wide EVOH film thickness distribution and possible existence of microcracks.

Since the barrier properties of monolayer EVOH films were inconclusive, three layers (LDPE|EVOH|LDPE) films were produced with an EVOH layer thickness comparable to commercial food packaging films (around $7\ \mu\ m$). The use of two external layers of

LDPE, as happens in commercial films, is expected to guarantee the required bubble stability, making it possible to obtain consistent barrier properties.

Anyway, monolayer films provided some relevant information concerning the inherent ability of the different types of particles to be dispersed and distributed in a EVOH matrix. From the overall analysis of monolayer micro and nanocomposite films, the NC and MCC particles showed a better dispersion. The MCC particles, when compared to CNC, had better thermal stability upon
extrusion, and consequently originate less degradation and better bubble stability during extrusion. SiO_2 nanoparticles, have a tendency to migrate to the film surface, a phenomenon that increases as the particle content increases. In general, it has been noticed that all composites show a tendency to form agglomerates on the surface of the polymer film, due to their high surface area, as also stated by Gashti et al. (2013). [40]

2 | Three-layer LDPE/EVOH/ LDPE films

Despite the already mentioned incompatibility between LDPE and EVOH, the separation of the film layers was only achieved when fracturing the films after immersion in liquid nitrogen, for SEM analysis. This test was performed to measure the thickness of each layer, as depicted in Figure 3. The thickness of the EVOH layer and of its micro and nanocomposites was in the range of $7.4-7.5\mu\ m$, value typically used in commercial flexible films. [1] The difficulty in separating the layers can be an indication of more reliable OTR results, as the EVOH is protected against humidity by the LDPE side layers.

Small angle X-ray scattering and XRD were performed to assess the dispersion of the NC and MCC particles and the results are depicted in Figures 4 and 5. On the diffractogram of the pure NC, Figure 4, a peak at $2\theta=1.8^{\circ}$ (d-spacing 49 Å) can be noticed. Through the SAXS pattern of the NC masterbatch, it was possible to observe that the d-spacing and visible wave amplitude
were maintained, possibly due to the high amount of NC used. For multilayer films with NC, SAXS patterns do not show any peak, which can indicate a higher intercalation or even exfoliation of NC platelets throughout EVOH matrix. [41]

The MCC XRD pattern, shown in Figure 5, presents a characteristic peak at $2\theta=22.7$ (d-spacing 3.91 Å), a value close to that reported in the study by Goo et al. (2021) that shows a characteristic peak at $2\theta=21^{\circ}$ for MCC Vivapur 105. For the MCC masterbatch, the characteristic peak of MCC moved to lower angles ($20=21.9^{\circ}$)

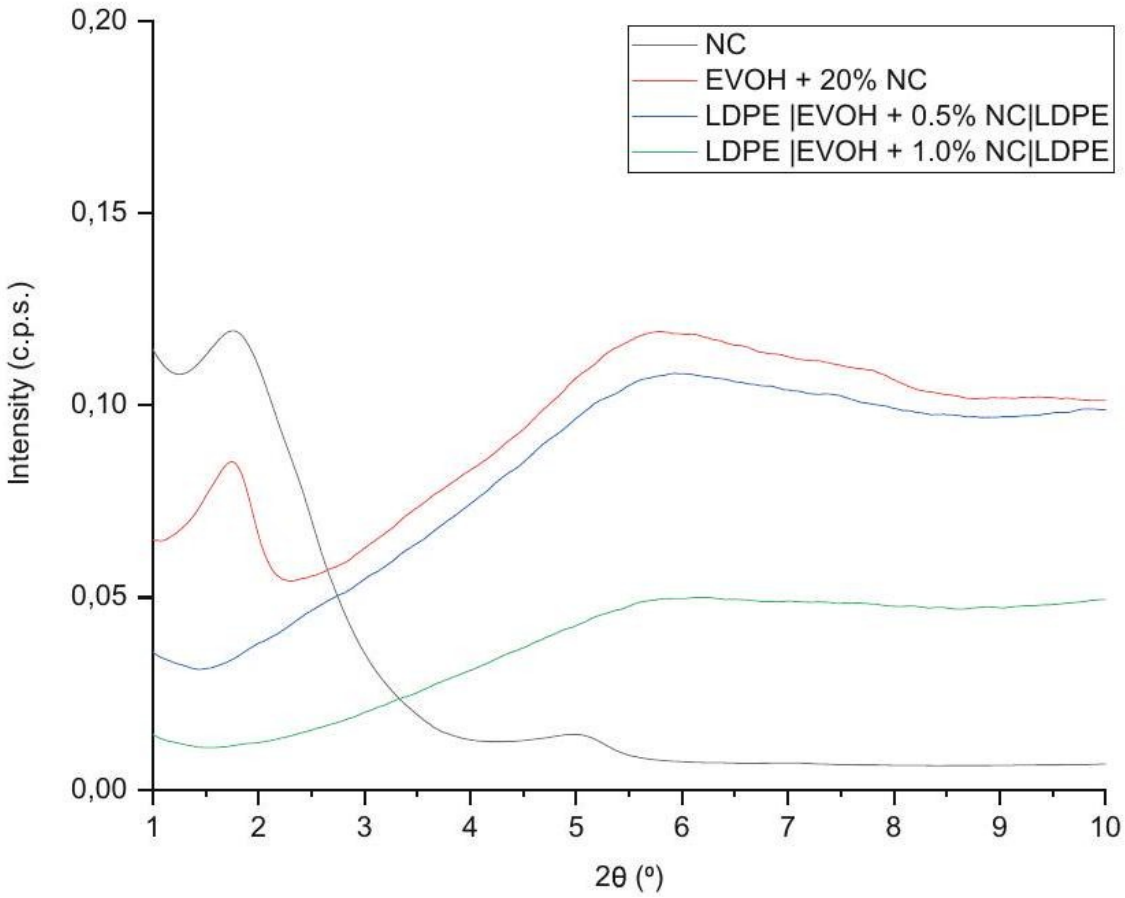

FIGURE 4 SAXS patterns of NC, and films with NC incorporation. [Color figure can be viewed at wileyonlinelibrary.com]

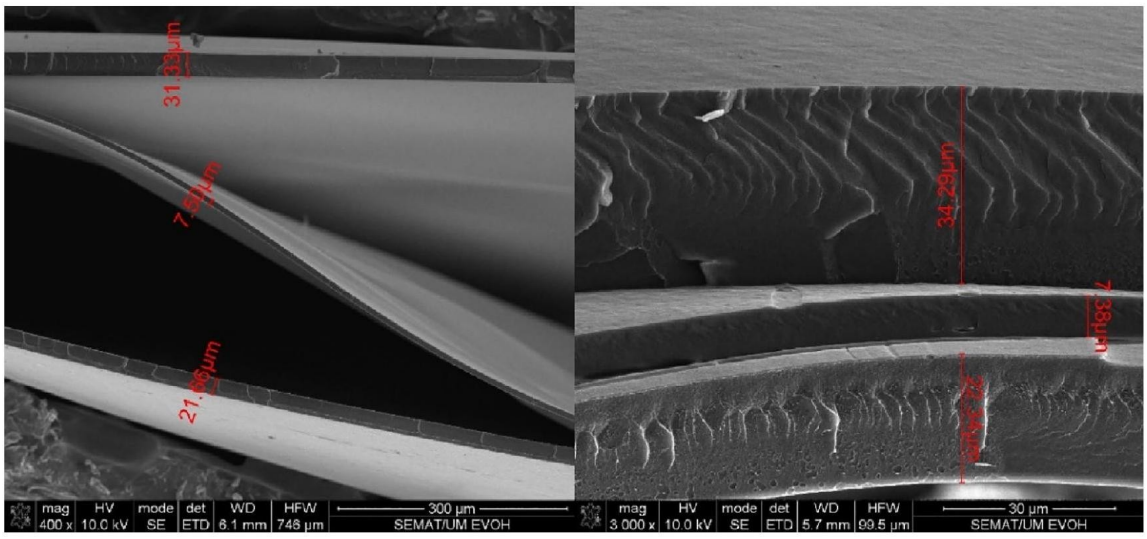

FIGURE 3 SEM micrographs of LDPE|EVOH|LDPE multilayer film. [Color figure can be viewed at wileyonlinelibrary.com]

leading to an increase in d-spacing to 4.06 Å.[42] Similarly to the multilayer NC films, in

these MCC multilayer films, the characteristic peak of MCC disappears, and it is only possible to observe the characteristic peaks of EVOH at $2\theta = 20.1^{\circ}$ and LDPE at 2θ of 21.4° 23.7° and 36.1° corresponding to the 110,200,020 lattice planes of the orthorhombic crystalline form of PE. [43–47]

The optical properties of the multilayer films (Table 4) with an inner layer of EVOH with incorporation of NC and MCC, have a slightly higher turbidity, which increases with wt. % of the particles incorporation, as it would be expected from the results obtained for the monolayer EVOH films (Table 3). Therefore, the best film is the one that incorporates $0.5\,wt.\,\%NC$. The incorporation of EVOH composites in the inner layer did not affect the brightness of the films, since its surface was the same as in the base film, composed by LDPE.

The OTR results, in Table 5, show that all the films with particles have better oxygen barrier than the base film, specially the films measured at $60\,\%RH$. The film with $1.0\,wt.\,\%NC$ achieved an OTR reduction of $45.3\,\%$ ($0\,\%RH$) and $29.0\,\%(60\,\%RH)$ when compared to the base

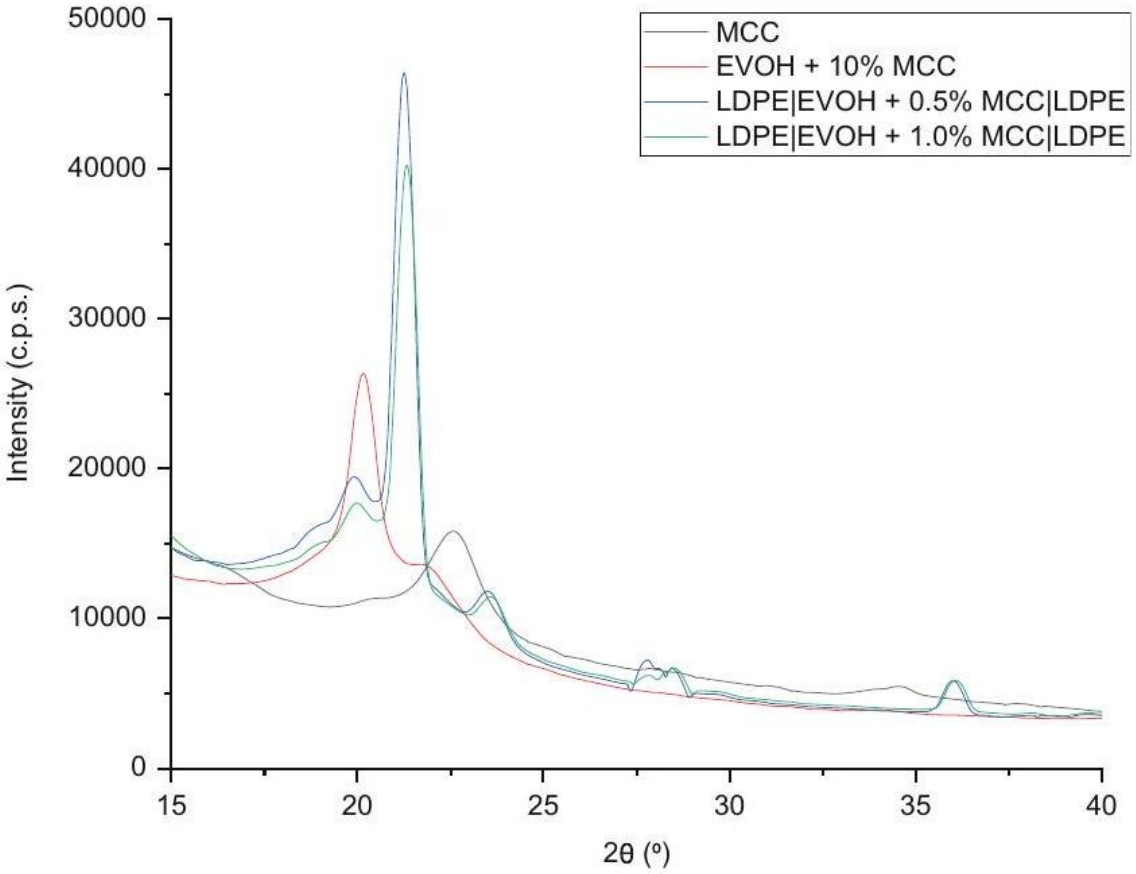

FIGURE 5 XRD patterns of MCC and films with MCC incorporation. [Color figure can be viewed at wileyonlinelibrary.com]

film. However, the statistical comparison of results at 0% RH , reveals that there are no significant differences among them. Nonetheless, for the tests performed at 60 % RH , the films with $0.5\,wt.\,\%NC$ and $1.0\,wt.\,\%MCC$ obtained significantly different OTR

values when compared to the base film. These are promising results for the flexible packaging film industry, as they allow to reduce the EVOH layer thickness while keeping the barrier properties of the packaging film.

The incorporation of particles did not affect the WVTR ($0.05 \pm 0.00 \ \ g/m^2 \ h$) of the control film. This is not surprising since the outer layers of the films are all composed by LDPE, a hydrophobic polymer. However, these results are interesting since no adhesive layer was used between the incompatible LDPE and EVOH layers.

4 | CONCLUSIONS

Ethylene vinyl alcohol masterbatch containing various types of micro and nanoparticles (NC, MCC, CNC, and SiO_2) were produced and used for the production of mono- and multilayer films. The NC masterbatch was able to incorporate 20 wt % of these particles at a

TABLE 5 OTR of multilayer films with LDPE, EVOH and respective micro and nanocomposites.

Multilayer Film samples	OTR (cm^3/m^2 day) $23^\circ C$; 0% RH	OTR (cm^3/m^2 day) $23^\circ C$; 60 % RH
LDPE|EVOH|LDPE	0.777 ± 0.127^{A}	0.672 ± 0.029^{A}
LDPE|EVOH +0.5% NC| LDPE	0.526 ± 0.135^{A}	0.399 ± 0.140^{B}
LDPE|EVOH +1.0% NC| LDPE	0.425 ± 0.044^{A}	0.477 ± 0.021^{AB}
LDPE|EVOH +0.5% MCC| LDPE	0.705 ± 0.146^{A}	0.439 ± 0.080^{AB}
LDPE|EVOH +1.0% MCC| LDPE	0.565 ± 0.204^{A}	0.436 ± 0.078^{B}

Note: Values that do not share a letter are significantly different.

Multilayer Film samples	Haze (%)	Gloss (60°)	Gloss (20°)
LDPE|EVOH|LDPE	7.9 ± 0.2^{C}	96.4 ± 1.4^{A}	9.80 ± 6.8^{A}
LDPE|EVOH +0.5% NC|LDPE	7.5 ± 0.4^{D}	94.4 ± 3.5^{A}	14.1 ± 3.8^{A}
LDPE|EVOH +1.0% NC|LDPE	8.3 ± 0.1^{B}	90.7 ± 7.8^{A}	11.8 ± 7.8^{A}
LDPE|EVOH +0.5% MCC|LDPE	8.5 ± 0.2^{AB}	92.5 ± 2.4^{A}	15.6 ± 2.5^{A}
LDPE|EVOH +1.0% MCC|LDPE	8.8 ± 0.2^{A}	88.3 ± 13.8^{A}	11.0 ± 9.6^{A}

Note: Values that do not share a letter are significantly different.

TABLE 4 Haze and Gloss of multilayer films with LDPE, EVOH and respective micro and nanocomposites.

temperature of $210^{\circ}C$. For the other particles, the incorporation rate was limited to $10\,wt.\%$, and a lower temperature (180 and $190^{\circ}C$) was used. This was due to nonsteady extrusion in the case of SiO_2 and thermal degradation in the case of CNC and NC. Microscopy revealed that NC showed better dispersion and distribution in the EVOH monolayer films at all incorporation rates. In terms of cellulose particles, CNC formed larger agglomerates compared to MCC, resulting in more unstable film extrusion and frequent rupture of the extruded bubble. Based on these findings, two types of particles, MCC and NC, were selected for the production of three-layer films. The results showed that the external LDPE layers provided excellent stability during the blown film process. The films had relatively low haze, allowing for good visibility of the food content, while their gloss was determined by the outer LDPE layers. The WVTR remained similar for all films, which can be attributed to the outer LDPE layers as well. Although the OTR results at 0% RH did not vary significantly, films with $0.5\,wt.\%NC$ and $1.0\,wt.\%$ MCC exhibited significantly lower OTR values compared to the base film at $60\%RH$.

Overall, the results suggest that incorporating low amounts of NC and MCC in an EVOH matrix has the potential to be implemented in the production of high barrier food packaging films with a reduced EVOH layer thickness. This would facilitate recycling of the multilayer films without compromising their performance during use.

AUTHOR CONTRIBUTIONS

Carolina Barros: Investigation (lead); methodology (lead); writing - original draft (lead). Ana G. Azevedo: Data curation (equal); formal analysis (equal); validation (equal). Miguel A. Cerqueira: Data curation (equal); formal analysis (equal); validation (equal). O. S. Carneiro: Conceptualization (equal); investigation (equal); methodology (equal); supervision (lead); validation (lead); visualization (lead); writing - review and editing (lead). A. V. Machado: Conceptualization (equal); methodology (equal); supervision (lead); validation (lead); visualization (lead); writing - review and editing (lead).

ACKNOWLEDGMENTS

This study was supported by the "BETTER PLASTICS PLASTICS IN A CIRCULAR ECONOMY" project, Reference POCI-01-0247-FEDER-046091.

FUNDING INFORMATION

This research was funded with European Union financial support, FEDER, through Competitiveness and Internationalization Operational Program (POCI) and Lisbon Operational Program (PO Lisbon).

CONFLICT OF INTEREST STATEMENT

The author(s) declare(s) that there is no conflict of interest.

DATA AVAILABILITY STATEMENT

The data that support the findings of this study are available on request from the corresponding author. The data are not publicly available due to privacy or ethical restrictions.

ORCID

Carolina Barros © https://orcid.org/0000-0003-4586-4374
Ana G. Azevedo © https://orcid.org/0000-0003-4671-2081
Miguel A. Cerqueira © https://orcid.org/0000-0001-66143942
O. S. Carneiro © https://orcid.org/0000-0001-5384-0028
A. V. Machado © https://orcid.org/0000-0003-1947-8605

REFERENCES

[1] N. Alipour, U. W. Gedde, M. S. Hedenqvist, S. Yu, S. Roth, K. Brüning, A. Vieyres, K. Schneider, Eur. Polym. J. 2015, 64, 36.
[2] Z. Tartakowski, Resour. Conserv. Recycl. 2010, 55, 167.
[3] M. Paul, B. Morris, J. Weinhold, K. Hausmann, J. Plastic Film Sheet. 2022, 38, 351.
[4] Z. Stelle, Minimum Standard for Determining the Recyclability of Packaging Subject to System Participation Pursuant to Section 21 (3) VerpackG (Verpackungsgesetz - Packaging Act). 2019.
[5] RECOUP, Plastic Packaging Recyclability By Design, RECOUP, Cambridgeshire, UK 2021.
[6] Recyclass, Recyclability Methodology Version 2.1, Recyclass, Belgium 2022.
[7] J. H. Chen, J. G. Liu, T. Q. Yuan, R. C. Sun, J. Appl. Polym. Sci. 2017, 134, 1.
[8] M. Vähä-Nissi, H. M. Koivula, H. M. Räisänen, J. Vartiainen, P. Ragni, E. Kenttä, T. Kaljunen, T. Malm, H. Minkkinen, A. Harlin, J. Appl. Polym. Sci. 2017, 134, 2.
[9] M. Alexandre, P. Dubois, Mater. Sci. Eng. Reports: A Rev. J. 2000, 28, 1.
[10] K. Müller, E. Bugnicourt, M. Latorre, M. Jorda, Y. Echegoyen Sanz, J. M. Lagaron, O. Miesbauer, A. Bianchin, S. Hankin, U. Bölz, G. Pérez, M. Jesdinszki, M. Lindner, Z. Scheuerer, S. Castelló, M. Schmid, Nanomaterials 2017, 7, 47.
[11] A. D. d. Oliveira, C. A. G. Beatrice, Nanocompos. Recent Evolutions. 2019, 103. https://doi.org/10.5772/intechopen. 81329
[12] B. Melendez-rodriguez, S. Torres-giner, L. Zavagna, C. Sammon, L. Cabedo, C. Prieto, J. M. Lagaron, Polymers 2021, 13, 2061.
[13] B. Podolyák, D. Kun, K. Renner, B. Pukánszky, Int. J. Biol. Macromol. 2018, 107, 1203.
[14] J. R. Wagner, B. Film, C. Film, Multilayer Flexible Packaging: Second Edition, Elsevier Inc., Oxford 2016, p. 137.
[15] M. Rahnama, A. Oromiehie, S. Ahmadi, I. Ghasemi, Polym. Sci. Ser A. 2017, 59, 533.
[16] Y. Liu, Y. Liu, S. Wei, Processing technologies of EVOH/nanoSiO2 high-barrier packaging composites, 17th IAPRI World Conference on Packaging, Tianjin, China 2010,

p. 269.
[17] G. Graninger, S. Kumar, G. Garrett, B. G. Falzon, Compos. Part A: Appl. Sci. Manuf. 2020, 139, 106103.
[18] E. Garofalo, P. Scarfato, L. Di Maio, L. Incarnato, Polym. Compos. 2018, 39, 3157.
[19] P. Scarfato, L. Di Maio, M. R. Milana, S. Giamberardini, M. Denaro, L. Incarnato, Food Addit. Contam. Part A Chem. Anal. Control. Expo. Risk Assess. 2017, 34, 1730.
[20] L. Cabedo, E. Giménez, J. M. Lagaron, R. Gavara, J. J. Saura, Polymer 2004, 45, 5233.
[21] S. Seethamraju, P. C. Ramamurthy, G. Madras, Royal Soc. Chem. 2013, 3, 12831.
[22] S. W. Kim, S. H. Cha, Appl. Polym. Sci. 2013, 8, 131.
[23] N. Gray, Y. Hamzeh, A. Kaboorani, A. Abdulkhani, Ind. Crops Prod. 2018, 115, 298.
[24] A. Kaboorani, N. Gray, Y. Hamzeh, A. Abdulkhani, Y. Shirmohammadli, Polym. Test. 2020, 93, 11.
[25] S. Liu, X. Li, L. Chen, L. Li, B. Li, J. Zhu, X. Liang, Carbohydr. Polym. 2017, 173, 143.
[26] C. Swaroop, M. Shukla, Int. J. Biol. Macromol. 2018, 113, 729.
[27] Y. Huang, L. Mei, X. Chen, Q. Wang, Nanomaterials 2018, 8,1.
[28] C. Vasile, Review 2018, 11, 1834.
[29] H. Zhang, C. Li, J. Guo, L. Zang, J. Luo, J. Nanomater. 2012, 2012, 1.
[30] N. Wu, Z. Luo, Y. Ge, P. Guo, K. du, W. Tang, W. du, A. Zeng, C. Chang, Q. Fu, J. Pharm. Anal. 2016, 6, 157.
[31] D. J. Voorn, W. Ming, A. M. van Herk, Macromolecules 2006, 39, 2137.
[32] Y. Zare, K. Y. Rhee, D. Hui, Compos. B Eng. 2017, 122, 41.
[33] K. M. A. Kaiser, J. Ewender, F. Welle, Polymers 2020, 12, 2988.
[34] V. Khoshkava, M. R. Kamal, Powder Technol. 2014, 261, 288.
[35] S. P. Bangar, M. M. Harussani, R. A. Ilyas, A. O. Ashogbon, A. Singh, M. Trif, S. M. Jafari, Food Hydrocolloids 2022, 130, 107689.
[36] F. A. Santos, G. C. V. Iulianelli, M. I. B. Tavares, Polym. Test. 2017, 61, 280.
[37] J. Markarian, Plast. Addit. Compd. 2007, 9, 32.
[38] M. Yao, J. Nan, T. Chen, Desalination 2014, 354, 116.
[39] G. A. Mountain, C. D. Keating, Meth Enzymol 2021, 646, 115.
[40] M. P. Gashti, H. Allahyary, P. Nasraei, M. P. Gashti, Fibers and Polym. 2013, 14, 1870.
[41] A. Babaei, S. R. Ghaffarian, M. M. Khorasani, S. Baseghi, J. Macromole. Sci. Part B. 2012, 51, 481.
[42] Y. T. Goo, C. K. Sa, J. Y. Choi, M. S. Kim, C. H. Kim, H. K. Kim, Y. W. Choi, Int. J. Nanomed. 2021, 16, 1245.
[43] W. Du, W. Zhong, Y. Lin, L. Shen, Q. Du, Eur. Polym. J. 2004, 40, 1987.
[44] D. Depan, W. Chirdon, A. Khattab, Polymers 2021, 13, 1558.
[45] A. N. Shebani, A. J. Van Reenen, M. Meincken, J. Compos. Mater. 2009, 43, 1305.
[46] J. T. Yeh, W. H. Yao, Q. Du, C. C. Chen, J. Polym. Sci. Part B: Polym. Phys. 2005, 43, 511.
[47] N. Aktzi, Y. Nir, D. Wang, M. Narkis, A. Siegmann, Polym. Compos. 2001, 22, 710.

How to cite this article: C. Barros, A. G. Azevedo, M. A. Cerqueira, O. S. Carneiro, A. V. Machado, J. Appl. Polym. Sci. 2025, 142(2), e56343. https://doi.org/10.1002/app.56343